Engineering Journal of Qatar University, Vol. 1, 1988.

# "DESIGNING AIR INTAKE DUCTS FOR HIGH SPEED FLIGHT"

*By*

**Wafik A. Kamal,**
Associate Professor,
Faculty of Engineering,
Qatar University, Doha,
Qatar, Arabian Gulf.

&

**Anwar E.M. Anwar,**
Lt. Colonel,
Egyptian Air Force,
Egypt.

## ABSTRACT

A proven duct flow model is used to examine the influence of the intake duct geometric and inlet flow parameters on the pressure recovery performance of intake ducts for high speed flight. The geometric parameters include: the inlet parallel pipe length, the diffuser cone angle, the length of the faired transition from the pipe to diffuser cone as well as the degree of the fairing. The inlet flow parameters examined are: the boundary layer momentum thickness, the velocity profile shape and the turbulence level. The inlet parameter values used simulate those following a normal shock wave — turbulent boundary layer interaction inside the intake duct, i.e. they simulate the conditions at the inlet to the diffuser of a supersonic intake.

## 1. INTRODUCTION

The application of turbojet engines to the propulsion of aircraft at supersonic speeds requires inlet and induction systems which provide high pressure recovery, low external drag, favourable stability and good engine-matching performance characteristics over a wide range of Mach numbers. In the design of supersonic intakes it is a usual practice to precede the diffuser by a length of parallel-walled duct in which the transformation to subsonic flow — through a shock wave — takes place. The shock is thus swallowed into the intake, and is made to occur at the smallest cross-section. This leads to a reduction in shock compression losses, a reduction in the likelihood of separation under shock and a lower sensitivity of the shock position to changes in back pressure. Figure 1 shows a typical supersonic intake duct, together with the theoretical variations in static pressure and Mach number along its length.

In this paper, a reliable compressible flow model (1) which accounts for the turbulence level of the core flow as well as the three-dimensional nature of the

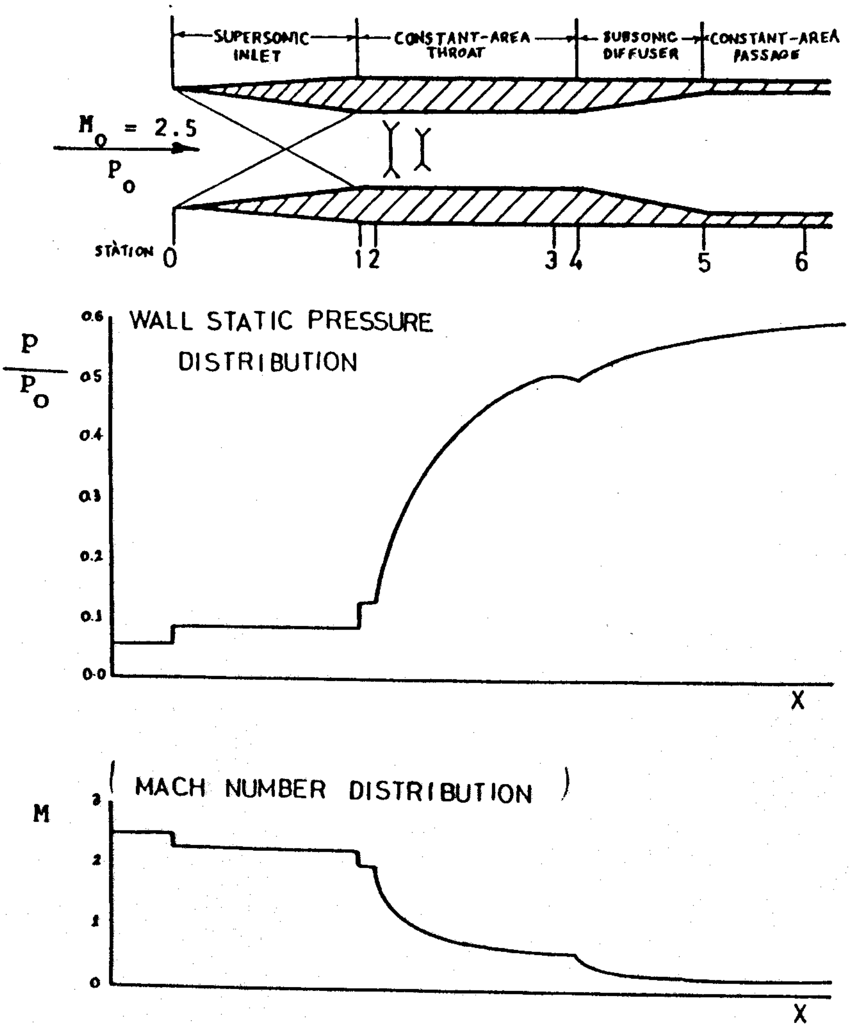


**Fig. 1: A Typical Supersonic Intake Duct.**

potential core is employed. The model is used to study the influence of each of the duct geometric parameters on its pressure recovery performance. Among these parameters are: the inlet pipe length, the diffuser cone angle, the effect of sharp transition from duct to diffuser or alternatively the effects of fairing the transition, and hence, the length and degree of fairing. The effects of varying the dominant intake flow parameters namely, the boundary layer thickness and shape parameter and the inlet turbulence level are also investigated.

Figure (2) shows a schematic drawing of the duct geometry considered. The duct length is divided into four regions namely, the inlet length EL, faired length FL, conical diffuser CL, and exit length XL.

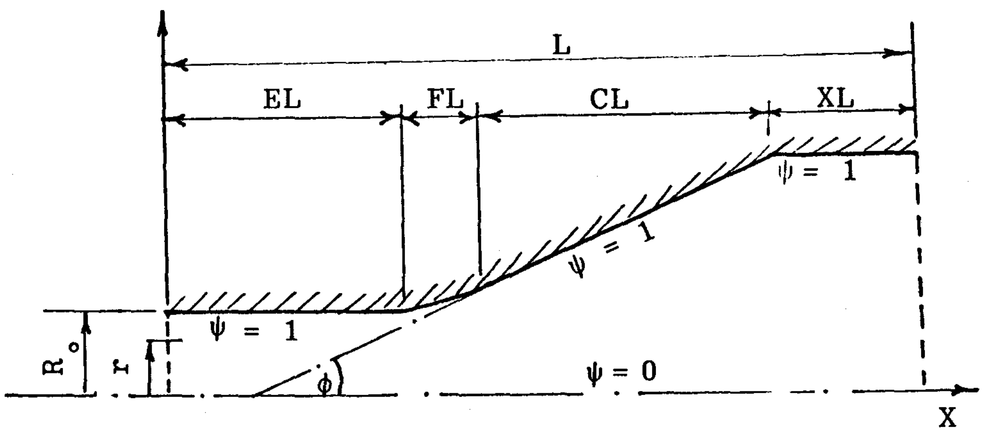


**Fig. 2: General Duct Geometry.**

## 2. MODEL EMPLOYED

The solution for the duct wall pressure distribution and total pressure loss as well as the variation of boundary layer parameters along the duct is obtained in three steps:-

i Solving the potential duct flow partial differential equations by an approximate method. This consists of expanding the stream function and the density function as power series in terms of the radius, thus reducing the inviscid flow equations to a series of simultaneous ordinary differential equations. The duct is divided into a number of points along its axis and the derivatives replaced by a finite difference representation. The resulting linear simultaneous algebraic equations are solved using an elimination algorithm.

ii Solving the boundary layer equations for the displacement thickness $\delta^*$ along the duct corresponding to the pressure distribution obtained from (i).

iii Resolving the potential flow equations with a modified wall shape to account for the boundary layer displacement.

Steps (ii) & (iii) are then repeated until the pressure distribution has converged to steady values.

## Formulation of Equations for the Potential Core Flow

For a compressible potential axisymmetric core flow the irrotationality equation can be written as (4)

$$RB \frac{\partial^2 \psi}{\partial R^2} + \frac{\partial^2 \psi}{\partial X^2} - R\left[\frac{\partial B}{\partial R} \cdot \frac{\partial \psi}{\partial R} + \frac{\partial B}{\partial X}\right] - B \cdot \frac{\partial \psi}{\partial R} = 0 \qquad (1)$$

in which

$\psi$ is the axisymmetric stream function defined using the boundary conditions

$\psi = 0$ on the axis & $\psi = 1$ on the duct wall (see Figure 1).

B is the density function defined as

$$B = \rho / \rho_o \qquad (2)$$

For an incompressible flow, equation (1) reduces to

$$\frac{\partial^2 \psi}{\partial X^2} + \frac{\partial^2 \psi}{\partial R^2} - \frac{1}{R} \cdot \frac{\partial \psi}{\partial R} = 0 \qquad (3)$$

which is Laplace's equation in cylindrical coordinates.

Because Equation (1) is an elliptic partial differential equation, either the values of $\psi$

or its derivatives must be known at all points on a closed boundary in order for a solution to be obtained. This is achieved by stipulating uniform flow in the axial direction at both entry and exit, with $\psi$ varying parabolically across the duct at either end between the values zero and one.

For a potential adiabatic (isentropic) axisymmetric flow, the energy equation can be written as

$$B^{\gamma-1} + \frac{\gamma-1}{2} M_o^2 \cdot \frac{1}{(2RB)^2} \left( \left(\frac{\partial\psi}{\partial R}\right)^2 + \left(\frac{\partial\psi}{\partial X}\right)^2 \right) = 1 + \frac{\gamma-1}{2} M_o^2 \quad (4)$$

The introduction of power series for the stream function $\psi$ and the compressibility function B allows the equations to be solved using direct elimination via a finite difference scheme. $\psi$ (X,R) & B(X,R) are expanded as the following power series:

$$\psi(X,R) = R^2 . f_1(X) + R^4 . f_2(X) + R^6 . f_3(X) + \ldots \quad (5)$$

$$B(X,R) = g_1(X) + R^2 . g_2(X) + R^4 . g_3(X) + \ldots \quad (6)$$

Note here that the term $B^{\gamma-1}$ in Equation (4) can be expanded in a binomial series as

$$B^{\gamma-1} = [1+(B-1)]^{\gamma-1}$$

$$= 1 + (\gamma-1)(B-1) + \frac{(\gamma-1)(\gamma-2)}{2} (B-1)^2 + \ldots \quad (7)$$

Then B is substituted from (6) into (7) before substituting it into equation (4). After the substitution (see reference (5)), it is found that all terms of the equation contain $R^{2n}$ while the right hand side of the equation is zero. Therefore, the coefficients of $R^{2n}$ must be zeros. This yields

$$\sum_{i=1}^{n} \left[ \varepsilon(n+1-i) \sum_{j=1}^{i} (g_{i+1-j} \cdot g_j) \right] - (1+w) \sum_{i=1}^{n} (g_i \; g_{n+1-i})$$

$$+ \frac{w}{4} \left[ \sum_{i-1}^{n-1} (f'_i \cdot f'_{n-1}) + 4 \sum_{i=1}^{n-1} i(n-i+1) \; f_i \cdot f_{n-i+1} \right] = 0 \quad (8)$$

in which $w = (\gamma - 1) M_o^2/2$

$\varepsilon$ (n) is the coefficient of $R^{2n}$ in the expansion of $B^{\gamma-1}$, given in reference (5) and the apostrophy sign denotes differentiation with respect to X.

Similarly, when the power series, Equations (5) & (6), are substituted into the irrotationality equation (1) and the coefficients of $R^{2n+1}$ are equated to zero, we obtain

$$\sum_{j=1}^{n} (g'_j \cdot f'_{n+1-j} - g_j \cdot f''_{n+1-j}) + \sum_{j=1}^{n+1} \left[4(n+2-j)(2(j-1)-n)\ g_j \cdot f_{n+2-j}\right] = 0 \qquad (9)$$

In both Equations (8) & (9) the derivatives (in the X-direction) are replaced by their finite difference representation using a Taylor series expansion. It is the solution of these two sets of equations, in finite difference form, together with the boundary condition that $\psi = 1$ on the wall, which gives the values of $f_i$ & $g_i$ for the stream function and density function in their respective power series expansions.

For a detailed account of the finite difference scheme as well as the iterative method of solving for the potential core pressure gradient, see reference (5).

**Formulation of the Boundary Layer Equations**

In this analysis, the boundary layer method developed by Kamal and Livesey (3) is employed. The method is based on the simultaneous solution of three equations for the boundary layer with the free stream velocity U being fed from the potential core flow solution. The boundary layer equations are:

**1. The momentum integral equation**

For a compressible axisymmetric boundary layer this may be stated in the form:

$$\frac{d\Theta}{dx} + \Theta\left[(2+H-M_e^2)\frac{d(\ln U)}{dx} + \frac{d(\ln R)}{dx}\right] = \frac{C_f}{2} + \frac{1}{\rho_e U^2} \cdot \frac{d}{dx}\int_0^{\delta} (\overline{\rho v'^2} - \overline{\rho u'^2})\,dy \qquad (10)$$

For the skin friction coefficient $C_f$ a modified version of the Ludwig-Tillman correlation is used, while for the Reynolds normal stress term (last term in Equation 10), three different correlations were attempted (3).

**2. The Entrainment Equation**

A compressible form of Head's entrainment equation can be written as:

$$H_1 \frac{d\theta}{dx} + \theta \frac{dH_1}{dx} = F - H_1 . \theta [(1-M_e^2) \frac{1}{U} \frac{dU}{dx} + \frac{1}{R} \frac{dR}{dx}] \quad (11)$$

in which $H_1 = 3.3 + 0.9/(\bar{H}-1)^{1.333}$

and $\bar{H} = (H+1)/(1+\frac{\gamma-1}{2}+r_e M_e^2) - 1$ ($r_e$ = temp. recovery factor)

**3. The Boundary Layer History Equation**

The turbulent kinetic energy integral equation is used to determine the streamwise evolution of the entrainment function F, thus

$$H_1 . \theta [\frac{1}{F} \frac{dF}{dx} + \frac{1}{U} \frac{dU}{dx} - \frac{1}{2R} \frac{dR}{dx}] = K_3 \sqrt{C_f/2} - F/2 \quad (12)$$

The value of $K_3 = 0.14$ is suggested.
(For the derivation of the above equations as well as a fuller account of the boundary layer model see Reference (3) )

The three boundary layer equations constitute a system of first order differential equations in $\theta$ , H and the turbulence determined entrainment function, F. Once $\theta$ & H are determined, the boundary layer displacement thickness, $\delta^*$ is calculated, the boundaries of the potential core are modified, and a new iteration is started until convergence is obtained.

**3. ANALYSIS OF EFFECTS ON DUCT GEOMETRY**

In this section, the duct inlet conditions are held at constant values, typical for those following a normal shock wave-turbulent boundary layer interaction (2). The study is made for three diffuser angles $5^0$, $12^0$ and $20^0$ chosen to represent typically a good diffuser (for which the theory should apply successfully), a practical diffuser and a wide angle diffuser respectively. The four geometrical parameters considered here are: the inlet length EL, faired length FL, degree of fairing D as well as the cone angle.

**Effects of Inlet Pipe Length, "EL"**

In Figures (3), (4) & (5) for the 5, 12 & $20^0$ diffusers respectively, with sharp transition, (FL=0), EL was varied from 2 to 6 times the inlet pipe radius. The figures indicate that, as EL increases a significant decay of the peaky inlet velocity profile takes place before the diffuser inlet section, i.e. the value of H at the diffuser inlet section becomes smaller. This results in a less disturbed and more uniform flow through the diffuser, delayed separation and a better diffuser performance. The negative value of $C_p$ at the sharp corner decreases as EL increases and consequently this leads to a higher $C_p$-maximum. Comparing Figures (3), (4) & (5) it can be concluded that the effects of varying EL are more pronounced for the larger diffuser angles.

**Effects of the Faired Length, "FL"**

Figures (6), (7) & (8) for the 5, 12 & $20^0$ diffusers show the effects of varying FL from 0 to 1 and 2. The figures suggest that the effects of FL are largely confined to the transition zone. An increase of FL leads to a favourable though slight decrease of the H-growth in the diffuser, thus delaying separation. Fairing the junction between the inlet pipe and diffuser cone eliminates the suction dip at the diffuser inlet and thus leads to an appreciable improvement in $C_p$ which extends to the diffuser exit. Increasing FL from 1 to 2 does not however seem to offer a significant improvement in the pressure recovery performance of the intake duct system.

**Effects of the Degree of Fairing, "D"**

The degree of the fairing, D is a factor in describing the duct geometry at the transition where the duct radius "r" is given by:

$$r = r_o + x^D$$

In Figures (9) to (11), the results for a sharp junction are compared to those for a faired junction with D=3, & D=5 for the three diffuser angles. The figures show that fairing the transition from the inlet pipe to diffuser cone slightly suppresses the boundary layer growth in the diffuser ($\theta$ & H) as well as eliminating the severe local negative then positive pressure gradients. The result is an appreciable improvement of the pressure recovery of the intake duct system. Trying different values of the degree of fairing indicated that a cubic fairing (D=3) gives the best results. This can

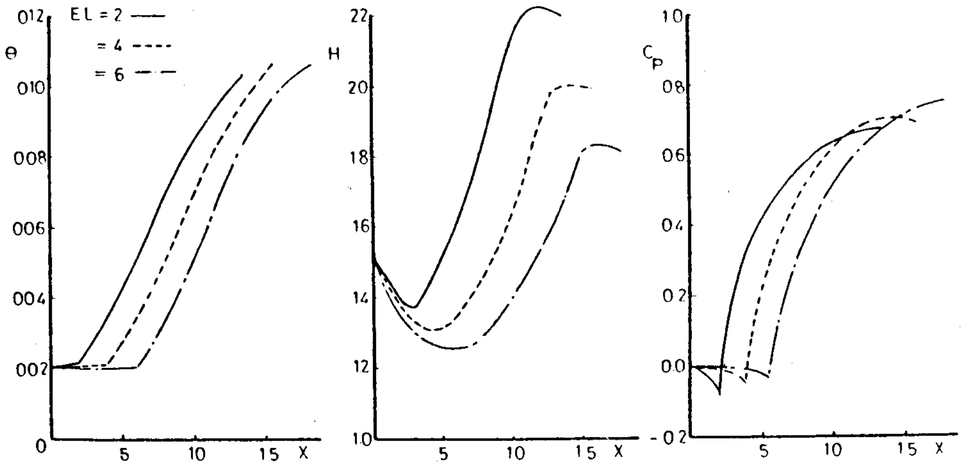


**Fig. 3: Effects of varying "EL" for 5⁰ Conical diffuser.**

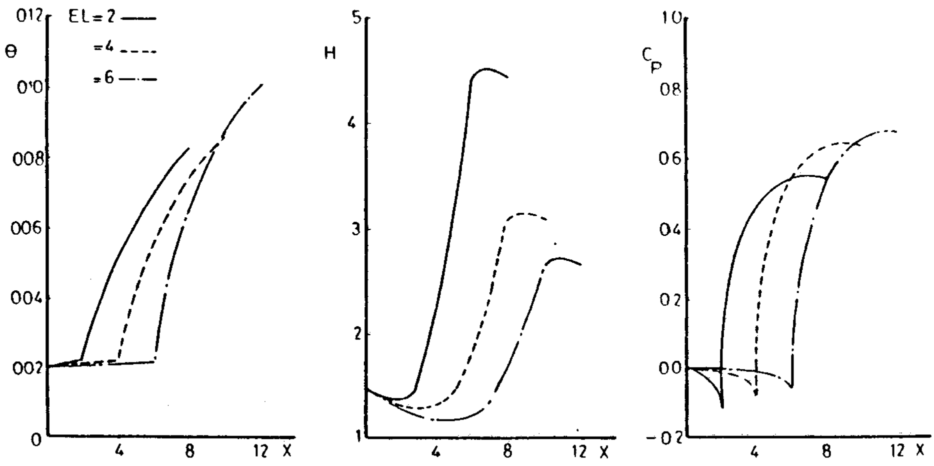


**Fig. 4: Effects of varying "EL" for 12⁰ Conical diffuser.**

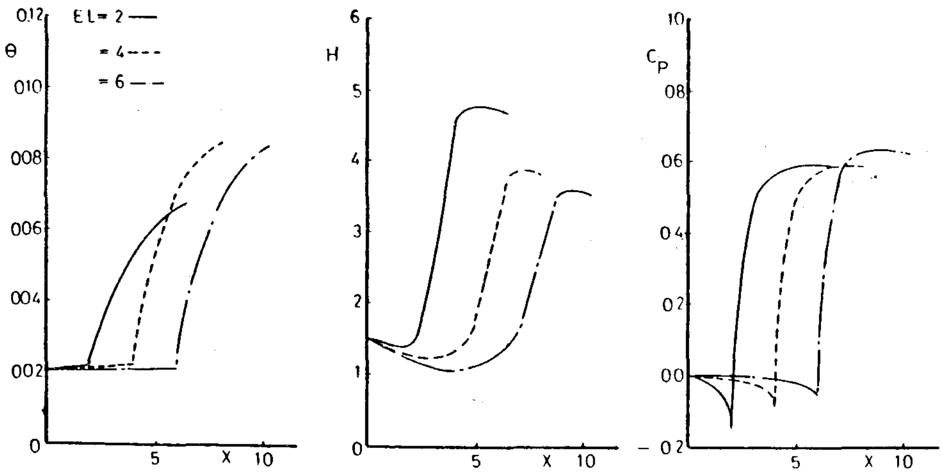


**Fig. 5: Effects of varying "EL" for 20⁰ Conical diffuser.**

be seen from comparing the curves for D=3 with those for D=5. Once again the effects of fairing the junction are more pronounced for the wider diffuser angles.

## 4. ANALYSIS OF THE EFFECTS OF INLET FLOW PARAMETERS

Kamal (3) has shown that a duct inlet flow situation can be adequately specified by means of five inlet flow parameters namely: the inlet Mach number $M_i$, Reynolds number Re and two boundary layer parameters e.g. the B.L. momentum thickness $\theta_i$ and the boundary layer velocity profile shape parameter $H_i$ in addition to a parameter quantifying the variation of the turbulence level across the inlet flow ($I_G$). $I_G$ is the mass-weighted turbulence intensity across the duct inlet section.

In this section, three diffusers of 5, 12 & $20^0$ included angles and of exit area ratio of 2 are considered. The diffusers have sharp transitions (FL = 0) and both the inlet and exit lengths are fixed at twice the inlet pipe radius (EL = XL = 2). The reference inlet flow conditions are $M_i = 0.7$, $Re = 10^6$, $\theta_i = 0.02$, $H_i = 1.4$ & $I_G = 6\%$. These values are varied when the particular inlet parameter is studied.

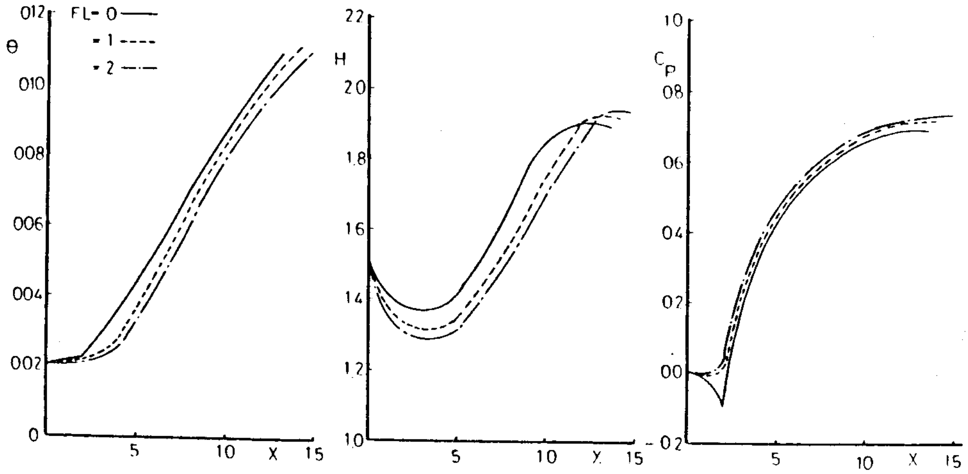


**Fig. 6: Effects of varying "FL" for 5⁰ Conical diffuser.**

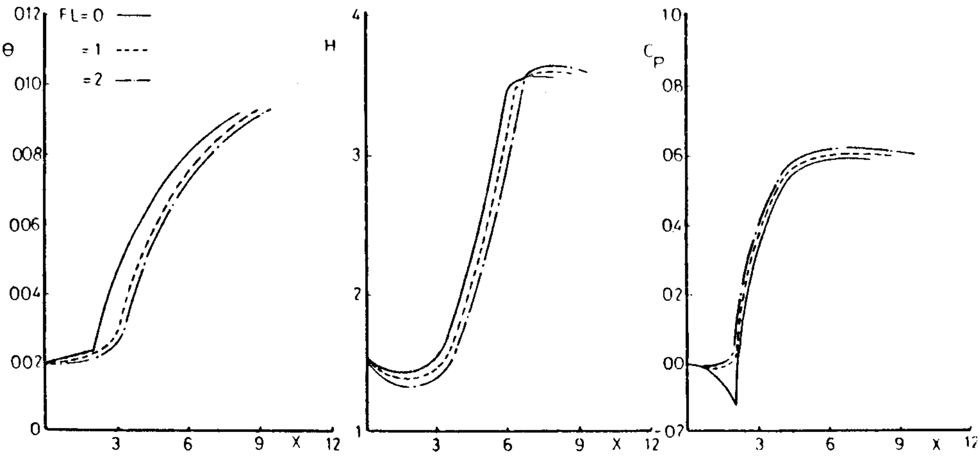


**Fig. 7: Effects of varying "FL" for 12⁰ Conical diffuser.**

229

*Designing Air Intake Ducts For High Speed Flight*

### Effects of Inlet Boundary Layer Momentum Thickness, "$\theta_i$"

In Figures (12) to (14) $\theta_i$ is varied from very thin to moderately thick. The figures show that an increase in $\theta_i$ increases slightly the rate of growth of $\theta$ in the diffuser but the effects on the H-growth are more pronounced. Thus an increase of $\theta_i$ leads generally to a decrease in the $C_p$-growth. Two more observations can be made from the curves for $C_p$. An increase of $\theta_i$ seems to increase the "cushioning effect" of the boundary layer on the sharp corner, thus reducing the local pressure depression. The theory also predicts the "Bradshaw Effect", i.e. the recovery in performance as $\theta_i$ approaches its fully developed pipe flow value. Surprisingly, this is correctly predicted while the value of the inlet turbulencparameter $I_G$ is held constant. For the $20^0$ diffuser, however, no "Bradshaw Effect" is evident.

### Effects of Inlet Velocity Profile Shape "$H_i$"

In Figures (15) to (17) for the three diffuser angles considered, the inlet velocity profile is varied from a developing profile (not yet fully developed) to a very peaky one, thus the $H_i$ values were 1.3, 1.5 & 1.7. The results indicate that $H_i$ is an influential diffuser inlet parameter. Increasing $H_i$ suppresses the $\theta$ growth in the diffuser, especially for the larger diffuser angles, but more significantly accentuates the rate of H-decay in the inlet pipe and the subsequent growth in the diffuser. The result is an appreciable deterioration in performance as the inlet profile becomes peakier, with separation shifting further upstream. Finally, it can be observed that at higher $H_i$ values the negative $C_p$ value at the sharp corner is suppressed. This is again attributed to an increase of the cushioning effect.

### Effects of Inlet Turbulence Level "$I_G$"

These are demonstrated in Figures (18), (19) & (20) for the 5, 12 & $20^0$ diffusers respectively. From the figures it can be observed that an increase in $I_G$ promotes the $\theta$ growth for the wider angle diffusers. However, the effects on velocity profile development in the diffuser is striking. Figure (18) suggests that, provided that the inlet turbulence intensity is high enough, a small angle diffuser can produce an outlet velocity profile which is more uniform than that at its inlet. This result is in line with the experimental results of Livesey & Turner (4) on diffusers with decaying inlet velocity profiles. It also provides the theoretical explanation needed. With the effects of $I_G$ on H-growth being much more significant than those on the $\theta$-growth, $C_p$ increases appreciably as the duct inlet turbulence level increases. Separation is also significantly delayed.

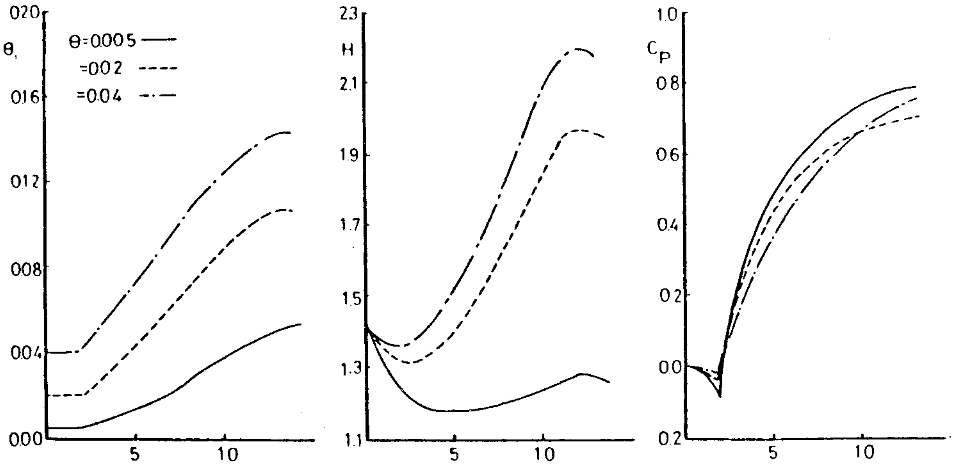


**Fig. 12: Effects of varying "E" for $5^0$ Conical diffuser.**

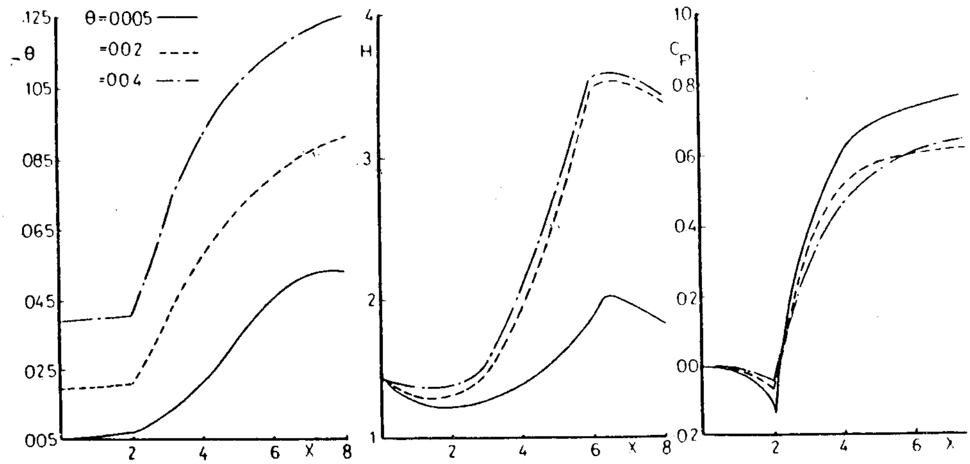


**Fig. 13: Effects of varying "O" for $12^0$ Conical diffuser.**

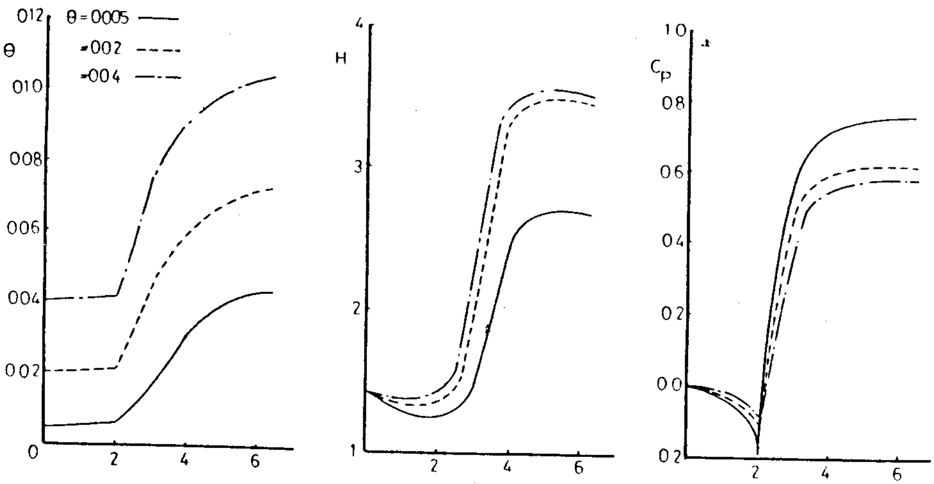


**Fig. 14: Effects of varying "O" for 20⁰ Conical diffuser.**

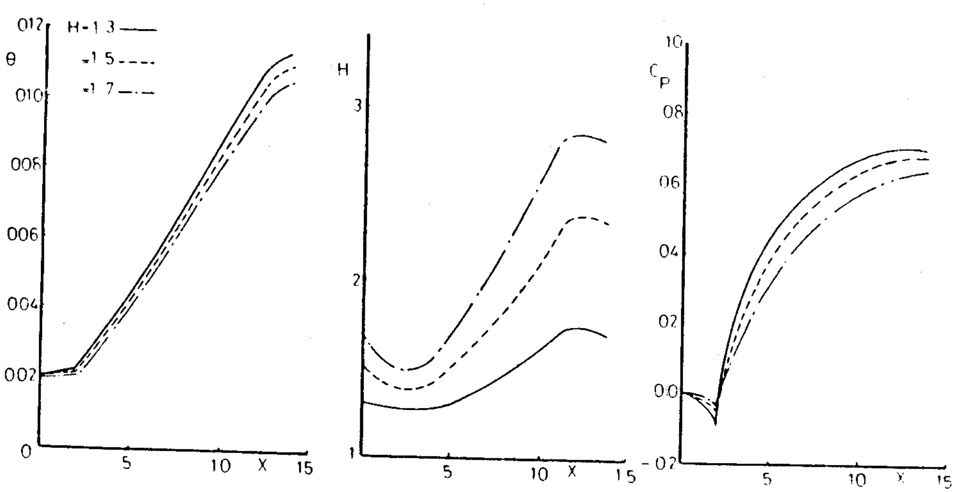


**Fig. 15: Effects of varying "H" for 5⁰ Conical diffuser.**

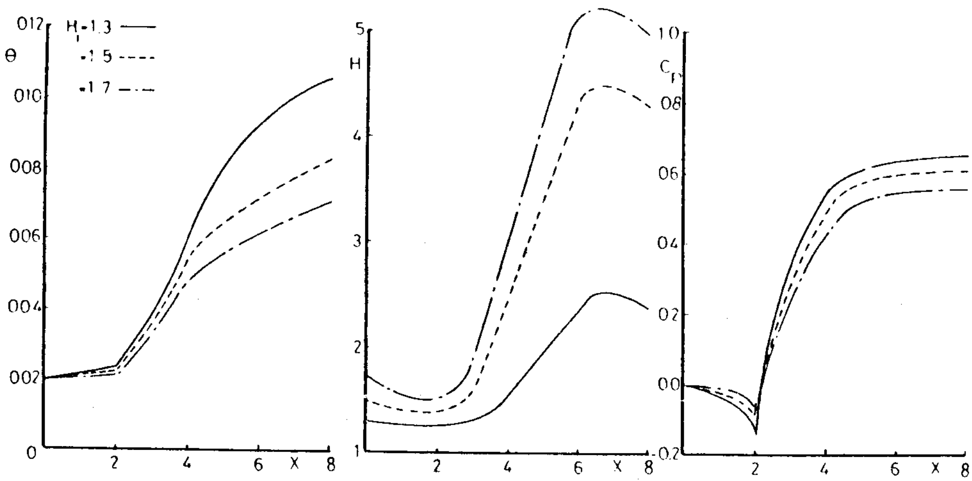


**Fig. 16: Effects of varying "H" for $12^0$ Conical diffuser.**

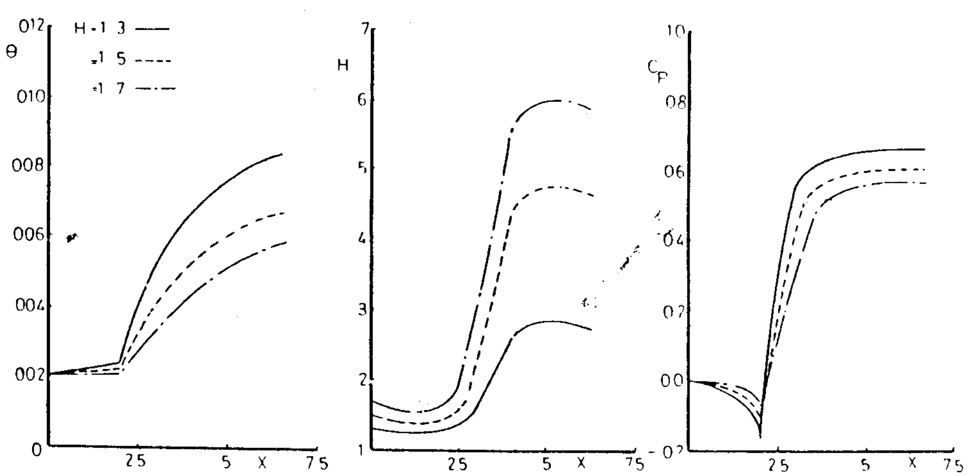


**Fig. 17: Effects of varying "H" for $20^0$ Conical diffuser.**

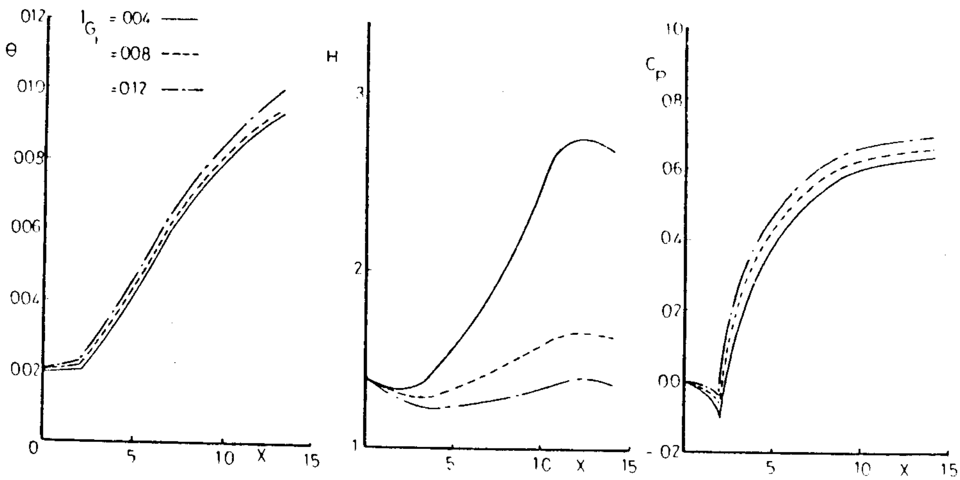


**Fig. 18: Effects of varying "$I_G$" for 5° Conical diffuser.**

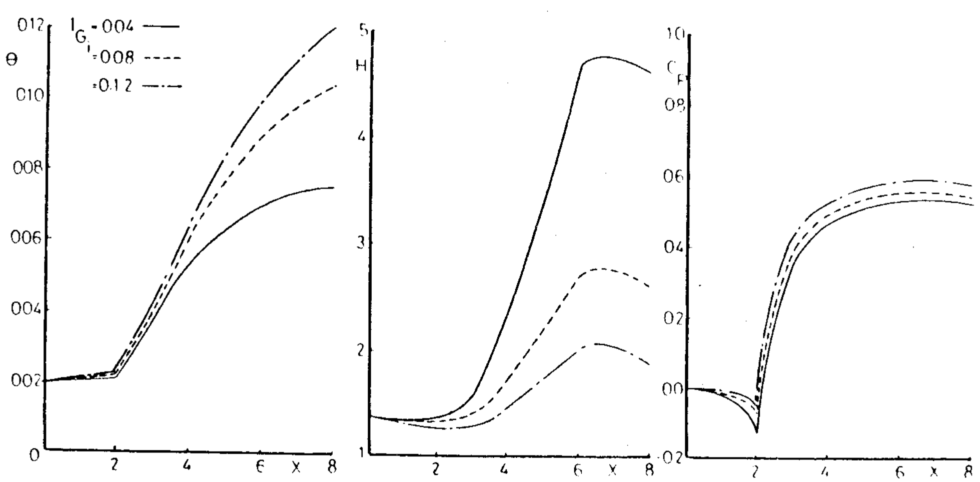


**Fig. 19: Effects of varying "$I_G$" for 12° Conical diffuser.**

## 5. CONCLUSIONS

Presented results indicate that, a well designed intake should contain no sharp corners, especially when wide angle diffusing parts are encountered. To eliminate the possibility of separation or stall the diffuser angle must not exceed $5^0$. However, a $12^0$ diffuser should experience no separation up to an area ratio of 2. Fairing the junction between the intake parallel pipe and the diffuser cone is essential. However, the length of the fairing is not an important design criterion. Normally a fairing length equal to one inlet duct radius is sufficient. The optimum fairing is that of the third degree, i.e. a cubic fairing.

Supersonic intake duct performance improves considerably as the inlet profile peakiness is decreased and the inlet turbulence level is increased. This is attainable by locating the shock wave-boundary layer interaction as early as possible in the intake duct, thus giving the flow more length to redistribute, with H decaying and $I_G$ increasing. The same conclusion was arrived at based on experimental evidence in reference (2).

## NOMENCLATURE

| | |
|---|---|
| B | density function, $= \rho / \rho_0$ |
| $C_p$ | wall static pressure recovery coefficient, $= (p-p_o)/(P_o-p_o)$ |
| EL,FL,XL | entry, faired and exit lengths / $r_o$ , see Figure 1 |
| F | entrainment function |
| $f_i$ , $g_i$ | nunctions of (X) defined by equations (5) & (6) |
| H | boundary layer shape factor, $= \delta^*/\theta$ |
| K | number of terms in the power series expansions of $\psi$ and B |
| M | local Mach number |
| P & p | local pressure, total & static |
| r | coordinate normal to duct axis |
| $r_o$ | duct radius at inlet |
| U | axial velocity at edge of the boundary layer |
| X,R | $x/r_o$, $r/r_o$ |
| x | coordinate along duct axis |
| $\gamma$ | ratio of specific heats |
| $\delta^*, \theta$ | displacement and momentum boundary layer thicknesses |
| $\rho$ | local density |
| $\psi$ | stream function |

## REFERENCES

1. **Kamal, W.A.** and **Anwar, A.:** "Modelling Compressible Flow in Axisymmetric Ducts of Varying Cross-Sectional Area", Proceedings of the First A.S.A.T., 14-16 May 1985, Cairo (1985).

2. **Kamal, W.A.** and **Livesey, J.L.:** "Diffuser Inlet Flow Following a Shock-Boundary Layer Interaction", Proceedings of the AIAA Fourth ISABE, Florida, U.S.A., April 1979, pp. 209-217, also AIAA Paper 79-7026 (1979).

3. **Kamal, W.A.** and **Livesey, J.L.:** "Prediction of Diffuser Flow and Performance Following a Normal Shock Wave-Turbulent Boundary Layer Interaction", Proceedings of the Symposium on Turbulent Shear Flows, The Pennsylvania State University, pp. 12.1-12.10 1(1977).

4. **Livesey, J.L.** and **Turner, J.:** "The Effect of Velocity Profile Decay on Shear Flow in Diffusers", Int. J. of Mech. Sciences, Vol. 6, pp. 371-377 (1964).

5. **Anwar, A.E.:** "Diffusers for Supersonic Intakes", M.Sc. Thesis, Alexandria University, (Oct. 1983).